

3-[¹²³I]Iodo- α -Methyltyrosine and [Methyl-¹¹C]-L-Methionine Uptake in Cerebral Gliomas: A Comparative Study Using SPECT and PET

Karl-J. Langen, Karl Ziemons, Jürgen C.W. Kiwit, Hans Herzog, Torsten Kuwert, Wolfgang J. Bock, Gerhard Stöcklin, Ludwig E. Feinendegen and Hans-W. Müller-Gärtner

Institute of Medicine and Institute of Nuclear Chemistry, Research Center Jülich, Jülich; Department of Nuclear Medicine and Department of Neurosurgery, Heinrich-Heine-University of Düsseldorf, Düsseldorf, Germany

This study compares the uptake of the nonmetabolizable amino acid analog 3-[¹²³I]iodo- α -methyltyrosine (IMT) and of [methyl-¹¹C]-L-methionine (MET) in cerebral gliomas. **Methods:** In 14 patients with cerebral gliomas, IMT uptake was measured using SPECT (10 dynamic, 4 static SPECT acquisitions) and, on the same day, MET uptake by dynamic PET. The IMT and MET data were compared with respect to tracer kinetics, tumor to brain ratios (T/B) and tumor size after converting the resolution of the PET scans to that of the SPECT scans (14 mm FWHM). **Results:** All gliomas showed increased uptake of both tracers in relation to normal brain tissue. Visual comparison of the scans yielded no differences in tumor size and shape with both methods. IMT showed a maximal tracer uptake in brain and in tumors at about 15 min postinjection which was followed by a washout of $45.0\% \pm 13.5\%$ in gliomas (mean \pm s.d., $p < 0.001$, $n = 10$) and $35.3\% \pm 5.4\%$ in normal brain ($p < 0.001$, $n = 10$) at 60 min postinjection. MET concentration in tumor tissue or brain tissue between 15 and 60 min remained constant. T/B ratios of IMT SPECT and MET PET showed a significant correlation at 15 min postinjection ($r = 0.69$, $n = 10$, $p = 0.03$), a low correlation for the mean values of the scans from 15–60 min postinjection ($r = 0.54$, $n = 14$, $p = 0.05$) and no correlation at 60 min postinjection ($r = 0.09$, $n = 10$, n.s.). **Conclusion:** IMT and MET uptake in gliomas is similar in the early, transport dominated phase. There are some differences in tumor to brain ratios between both tracers within the first hour postinjection that are mainly caused by variable washout of IMT. Imaging of tumor extent with IMT SPECT is comparable to MET PET. Thus, amino acid SPECT using IMT is a promising tool to evaluate the biological activity and intracerebral infiltration of gliomas.

Key Words: amino acids; 3-[¹²³I]iodo- α -methyltyrosine; [methyl-¹¹C]-L-methionine; cerebral gliomas; SPECT; PET

J Nucl Med 1997; 38:517–522

Studies of the brain with radiolabeled amino acids show great potential for more accurate diagnosis of cerebral gliomas (1–6). Although cranial CT and MRI are unsurpassed diagnostic modalities for the detection of cerebral space-occupying lesions, the differentiation of tumor tissue from edematous, necrotic and fibromatous tissue with these methods is not optimal. PET with ¹⁸F-fluorodeoxyglucose is useful in estimating tumor grade and prognosis of gliomas (7), but the delineation of tumors is difficult because of high glucose metabolism in normal cortex.

Various PET studies have shown that accumulation of [methyl-¹¹C]-L-methionine (MET) spreads beyond the tumor margin as defined by CT and MRI and correlates with histological tumor spread (1–4,6). The role of amino acid accumulation in tumor grading, prognosis, detection of recurrence and

therapeutic response is still under investigation. The underlying mechanism of increased accumulation of large neutral amino acids in cerebral gliomas is not yet fully explained. On the one hand it is assumed that increased protein synthesis is the driving force; on the other hand, several studies have given rise to the assumption that transmembraneous transport phenomena play a major role in the uptake process (8–11). While brain imaging of amino acid uptake is easily performed with ¹¹C labeling and PET, tracers for SPECT are rarely available.

3-[¹²³I]iodo- α -methyltyrosine (IMT) is an amino acid analog initially tested for pancreas imaging and melanoma detection (12,13). Recent investigations have shown that:

1. IMT accumulates in brain tumors (14,15).
2. IMT, like other large neutral amino acids, is transported across the intact blood-brain barrier but not incorporated into cerebral proteins (15,16).
3. The uptake of IMT by normal brain and gliomas can be competitively inhibited by infusion of natural L-amino acids (17).

This study compares the results obtained by IMT-SPECT with those obtained by MET-PET in patients with cerebral gliomas. MET was chosen among the many amino acids labeled with ¹¹C for PET studies because most data in the literature are reported for MET. Since MET is a naturally occurring amino acid that is incorporated into protein, and IMT is an unphysiological amino acid that is assumed to participate in the same transport process (17,18) without being metabolized, this study gives some insight into the role of transport phenomena for the accumulation of large neutral amino acids in human gliomas. This study of 14 patients with cerebral gliomas compares the two modalities for tumor to brain ratios, tumor extent and tracer kinetics using dynamic PET and dynamic SPECT.

MATERIALS AND METHODS

Patients

Fourteen patients with cerebral gliomas, admitted consecutively to the department of neurosurgery who agreed to participate in the study, were investigated by IMT-SPECT and MET-PET. Clinical data concerning the group of patients are given in Table 1. Histopathological data were obtained by open surgery or stereotactic biopsy. After the patients had fasted overnight, the SPECT and PET investigations were performed on the same day, and food was withheld throughout both investigations. Because the gamma-radiation of ¹²³I does not interfere with the PET measurement, the IMT-SPECT studies were performed before the PET studies.

SPECT

IMT was prepared, as previously described, with a specific activity of >167 TBq/mmol (4500 Ci/mmol) (19). Thirty minutes before the SPECT study the patients received 900 mg sodium

Received Jan. 29, 1996; revision accepted Jul. 1, 1996.

For correspondence or reprints contact: Karl-Josef Langen, MD, Institute of Medicine, Research Center Jülich, P.O. Box 1913, 52425 Jülich, FRG.

TABLE 1
Patient Data

Patient no.	Age (yr)	Sex	Histopathology	Grade	Pretreatment	Contrast enhancement in CT or MRI	IMT-SPECT
1	61	M	Glioblastoma	IV	None	+++	Dynamic
2	58	M	Astrocytoma	II	Biopsy	+	Dynamic
3	54	M	Glioblastoma	IV	None	+++	Dynamic
4	54	F	Glioblastoma	IV	None	++	Dynamic
5	39	M	Astrocytoma	II	Biopsy	-	Dynamic
6	66	M	Glioblastoma	IV	None	+	Dynamic
7	48	M	Glioblastoma	IV	None	+	Dynamic
8	41	M	Oligodendroglioma	II	Surgery	-	Dynamic
9	30	M	Glioblastoma	IV	Irradiation	+++	Dynamic
10	61	F	Astrocytoma	II	None	-	Dynamic
11	54	F	Astrocytoma	II-III	None	++	Static
12	49	M	Glioblastoma	IV	None	+++	Static
13	53	M	Astrocytoma	III	Surgery	++	Static
14	58	M	Glioblastoma	IV	None	+++	Static

perchlorate to block possible uptake of free radioactive iodide by the thyroid. The SPECT studies were performed using a triple-head gamma camera system equipped with ultra-high resolution fan-beam collimators. Head movements were minimized by a plastic mask adapted to the patient's head before the studies. In 10 of the patients, dynamic SPECT acquisitions (8×2 min, 9×5 min) were started after a bolus injection of 370–550 MBq IMT, and in four of the patients only static SPECT scans from 15–60 min postinjection. Samples of arterialized venous blood were taken every 15–30 sec at the beginning with increasing time intervals up to 1 hr. Blood samples were centrifuged and aliquots of plasma were measured in a well counter. The well counter was cross-calibrated against the SPECT scanner using a brain phantom study. The SPECT data were reconstructed by filtered backprojection using a Butterworth filter (0.35 high cut, 3.0 roll off) and corrected for attenuation according to Chang (first order $\mu = 0.1$) (20) using a contour-finding procedure for each slice. No scatter correction was performed. The plasma input function was corrected for the non-IMT radioactivity using standard values (15).

PET

The PET studies were performed about 2 hr after the SPECT studies using a PET scanner with a 10.5 cm axial field of view (21). The procedure of positioning and fixation of the patient's head was identical to the SPECT studies. After transmission scans using a rotating $^{68}\text{Ga}/^{68}\text{Ge}$ source and a bolus injection of 740–1110 MBq MET, dynamic PET data were recorded for 60 min. Samples of arterialized venous blood were taken, and the radioactivity of plasma was corrected for non- ^{11}C -L-MET radioactivity using standard values (22). PET data were reconstructed by filtered backprojection and corrected for scattered radiation and attenuation. In order to make the spatial resolution and partial volume effects in PET and SPECT comparable, the reconstructed PET scans were smoothed to the resolution of the IMT-SPECT scans of about 14 mm by adapting the modulatory transfer function.

Data Analysis

The MET-PET scans were transferred to the SPECT computer system and adapted to the matrix size (64×64 pixels), pixel size (3.57 mm) and slice thickness (3.57 mm) of the SPECT scans. Identical position and rotation of the transaxial slices in the SPECT and PET studies was controlled by an overlay procedure. The MET-PET scans were then evaluated by irregular ROIs placed on the tumor in the transaxial slice with highest tracer accumulation and an area of normal brain according to a corresponding CT or MRI scan. These regions were transferred to the corresponding

IMT scans. Tumor to brain ratios of the radioactivity per milliliter of tissue at 15 min and 60 min postinjection from the data of the 10 patients who had dynamic scans and the mean values of the tumor to brain ratios from 15–60 min postinjection for all 14 patients including those patients who had only static SPECT scans were used to correlate IMT-SPECT and MET-PET data. For the evaluation of tumor spread, the MET PET scans and the IMT SPECT scans were summed up from 15–60 min postinjection and examined independently by three experienced nuclear medicine physicians.

Kinetic Analysis

In the 10 patients for whom a full set of dynamic data for SPECT and PET was available, tracer kinetic evaluations were applied to tissue and plasma time-activity data. The kinetic evaluations of IMT data were based on the assumption of a two-compartment model similar to the nonmetabolized amino acid analog [^{11}C] aminocyclohexanecarboxylate (23). The IMT data were analyzed by nonlinear least-square fits using K_1 , k_2 and cerebral blood volume (CBV) as fit parameters. Furthermore, k_3 was included to test the need for a third compartment representing metabolized radiotracer (23). For a two-parameter model, the ratio of the parameters K_1 and k_2 predicts the tissue volume of distribution (V_d).

Since for the evaluation of MET-PET data the extraction of rate constants for single compartments is crucial (24), the linearization procedure of Patlak (25) was used to determine the rate constant of net tracer influx, K_i , which includes tracer transport, protein incorporation and other intracellular binding. The rate constant of net tracer influx K_i is given by the slope of the linear part of this plot, the volume of distribution (V_d) by the y-intercept.

Statistical Analysis

Values are expressed as mean \pm s.d. Statistical methods used were Student's t-test or Mann-Whitney rank sum test for group comparisons and Pearson's correlation coefficient. Probability values less than 0.05 were considered significant.

RESULTS

An example of the kinetics of both IMT and MET in an astrocytoma Grade II, brain and plasma (Patient 10) is given in Figure 1. IMT showed a maximal tracer uptake in brain and in tumors at about 15 min postinjection that was followed by a tracer washout of $45.0\% \pm 13.5\%$ in gliomas ($p = 0.001$, $n = 10$) and $35.3\% \pm 5.4\%$ in normal brain ($p = 0.001$, $n = 10$) at 60 min postinjection (data not shown). For MET, there was no significant change in tracer concentration in tumor tissue or brain tissue between 15 and 60 min postinjection ($1.47\% \pm$

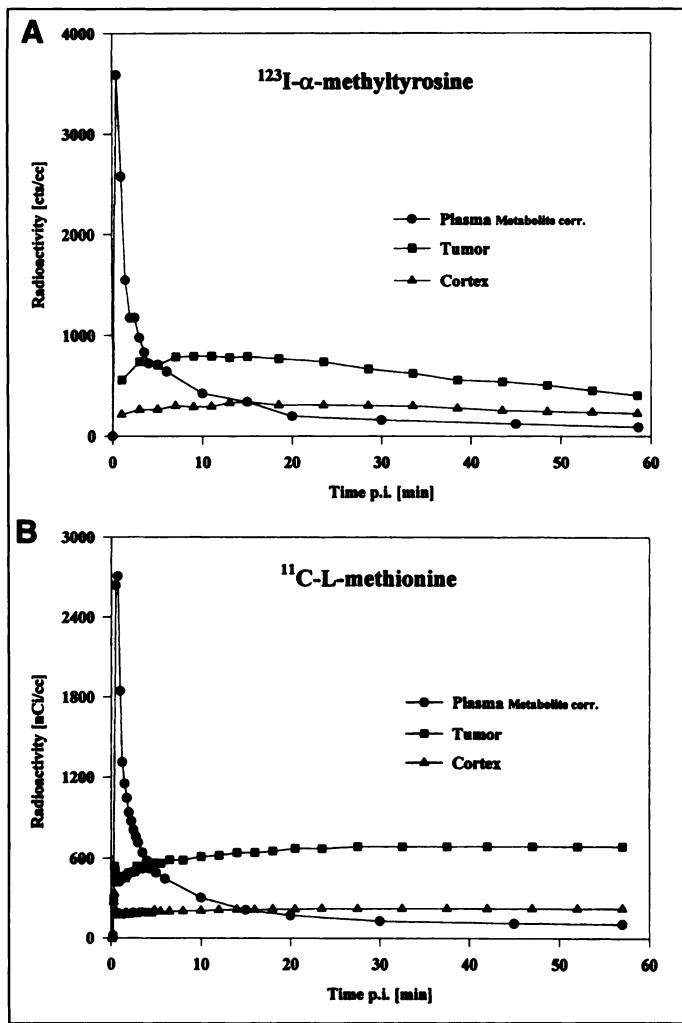


FIGURE 1. Kinetics of (A) ^{123}I - α -methyltyrosine and (B) ^{11}C -L-methionine in tumor, brain and plasma of Patient 1. For both tracers, radioactivity in the tumor and brain reaches a maximum at about 15 min postinjection that is followed by washout of IMT.

7.3%, respectively, $-0.97\% \pm 4.8\%$, $n = 10$, n.s., data not shown).

Data on tumor to brain ratios are given in Table 2. The tumor to brain ratios for IMT decreased significantly from 15–60 min postinjection (1.96 ± 0.42 versus 1.61 ± 0.29 , $n = 10$, $p < 0.05$) while there was no change for MET (2.34 ± 0.44 versus 2.30 ± 0.55 , $n = 10$, n.s.). The mean values of the tumor to brain ratios averaged between 15 and 60 min postinjection were significantly lower for IMT than for MET (1.77 ± 0.32 versus

TABLE 2
Tumor-to-Brain Ratios of IMT and MET

Patient no.	IMT-SPECT (Tumor/brain ratios)			MET-PET (Tumor/brain ratios)		
	15 min	60 min	mean	15 min	60 min	mean
1	1.37	1.43	1.40	1.99	1.78	1.89
2	1.99	1.13	1.56	1.90	1.79	1.84
3	2.15	1.41	1.78	2.98	3.20	3.09
4	1.31	1.50	1.40	1.88	1.83	1.86
5	2.66	2.23	2.44	2.51	2.02	2.27
6	2.08	1.74	1.91	2.23	2.21	2.22
7	2.00	1.57	1.78	2.62	2.78	2.70
8	1.63	1.70	1.67	1.88	1.87	1.87
9	2.04	1.60	1.82	2.39	2.40	2.39
10	2.32	1.81	2.06	3.02	3.13	3.08
11	—	—	1.52	—	—	1.70
12	—	—	1.53	—	—	1.96
13	—	—	1.58	—	—	2.09
14	—	—	2.29	—	—	2.42
mean	1.96	1.61	1.77	2.34	2.30	2.24
s.d.	0.42	0.29	0.32	0.44	0.55	0.45

$p < 0.05$

$p < 0.02$

2.24 ± 0.45 , $n = 10$, $p = 0.02$). Tumor to brain ratios of IMT SPECT and MET PET showed a significant correlation at 15 min postinjection ($r = 0.69$, $n = 10$, $p = 0.03$), a low correlation for the mean values of the scans from 15–60 min postinjection ($r = 0.54$, $n = 14$, $p = 0.05$) and no correlation at 60 min postinjection ($r = 0.09$, $n = 10$, n.s.; Fig. 2). The visual comparison of the IMT SPECT scans and MET PET scans yielded no obvious difference in tumor size and shape. Examples of IMT SPECT and MET PET scans of two patients with astrocytomas Grade II (Patients 5 and 10) are shown in Figures 3 and 4.

The K_1 values for IMT, the K_1 values for MET and V_d values for all 10 patients who had dynamic SPECT and PET scans are presented in Table 3. The nonlinear least-square fits to the IMT data using K_1 , k_2 and CBV as fit parameters yielded satisfactory fits to the data (Fig. 5). Addition of k_3 to the fit procedure yielded small values for k_3 (k_3 -tumors: 0.005 ± 0.006 , k_3 -brain: 0.004 ± 0.004 .) without a remarkable improvement of the fit.

An example of a Patlak plot to the MET data of tumor and brain of Patient 10 is shown in Figure 6. In all patients the Patlak plots to the MET kinetics in tumors and brain became linear within the time of measurement. The K_1 values for IMT were significantly higher for gliomas than for brain (0.044 ± 0.021 vs 0.020 ± 0.008 , $n = 10$, $p = 0.01$) as were the K_1 values

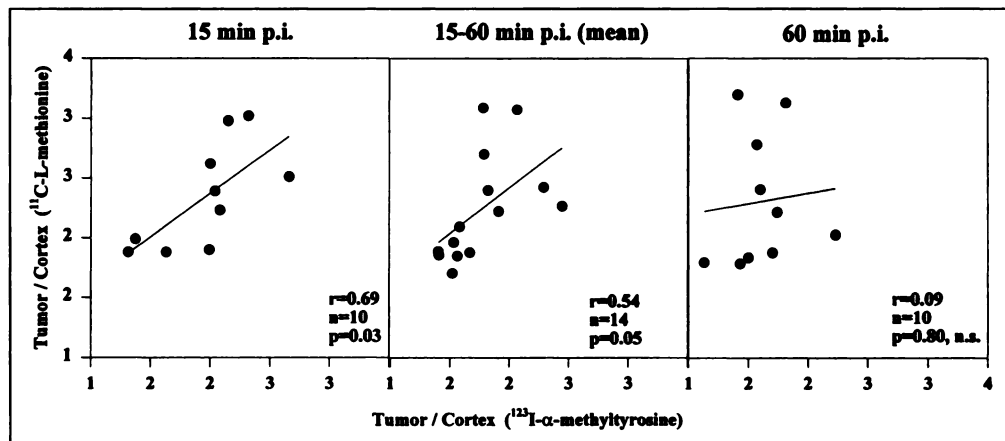


FIGURE 2. Comparison of tumor-to-brain ratios for IMT-SPECT and MET-PET. There is a significant correlation in the transport dominated phase at 15 min postinjection, a low correlation for the mean values of the scans from 15 to 60 min postinjection (including the four patients with static SPECT scans), but no correlation at 60 min postinjection

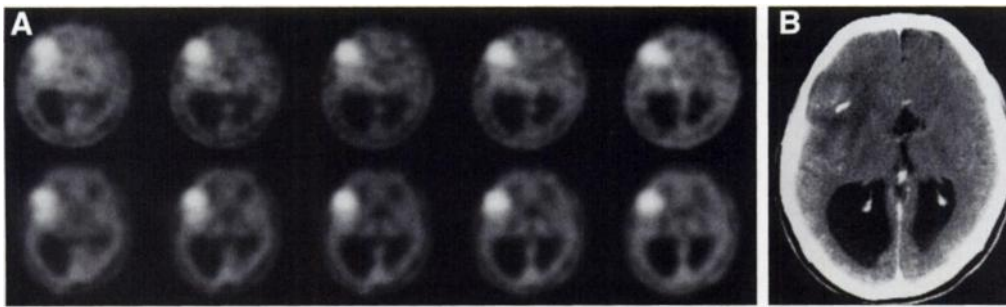


FIGURE 3. (A) Comparison of IMT-SPECT scans (upper row) and MET-PET scans (lower row) (15–60 min postinjection) in an astrocytoma Grade II (Patient 5). The extent of the tumor area with increased tracer uptake appears to be identical for IMT and MET. (B) The contrast-enhanced CT scan of Patient 5 shows no major contrast enhancement in the tumor area indicating that there is no blood-brain-barrier disruption.

for MET (0.044 ± 0.018 versus 0.019 ± 0.006 , $n = 10$, $p = 0.01$). The K_1 values for IMT and K_1 values for MET in the tumors showed a significant correlation ($r = 0.83$, $n = 10$, $p < 0.001$, Fig. 7). The V_d values for IMT were significantly higher for gliomas than for brain (0.94 ± 0.27 vs. 0.58 ± 0.13 , $n = 10$, $p = 0.01$) as were the V_d values for MET (1.07 ± 0.64 versus 0.45 ± 0.29 , $n = 10$, $p = 0.01$). There was no correlation between the V_d values for IMT and MET in the tumors.

DISCUSSION

This study was designed to further validate IMT as a SPECT tracer of amino acid uptake in brain tumors. In this comparative study, the amino acid MET was chosen as a reference because a similarity of the results for IMT and MET offered the chance to transfer the experiences with MET PET to the clinical application of IMT SPECT.

In addition, this study compares the intratumoral and intracerebral accumulation of two different large neutral amino acids, one of which (MET) is a natural amino acid and takes part in cellular metabolism while the other (IMT) is a synthetic amino acid that probably uses the same carrier system but is not incorporated into proteins. The comparability of IMT and MET results is confounded by methodological differences of SPECT and PET, but this is not a serious limitation in our opinion.

It was demonstrated that uptake of IMT and MET was increased in all gliomas in relation to normal brain tissue, and no conflicting results for the two tracers were observed. While MET concentration in the tumors and in the brain remained nearly constant between 15 and 60 min postinjection, IMT showed a significant washout. IMT washout was higher in the tumors than in the brain, and as a consequence the tumor to brain ratios decreased significantly from 15–60 min postinjection. This finding can be explained by a low intracellular binding of IMT and confirms experimental data that IMT is not incorporated into proteins (15,16). The lack of significant intracellular binding also was confirmed by the kinetic analysis of the IMT data. Nonlinear regression analysis of the IMT data using K_1 , k_2 and CBV as fit parameters yielded satisfactory fits to the data. Addition of k_3 to the fit procedure yielded only a minimal improvement of the fit and small values for k_3 , indicating no need for a third compartment representing metabolized tracer. These results are

similar to those reported for the nonmetabolized amino acid analog ^{11}C -aminocyclohexanecarboxylate (23).

The comparison of the tumor to brain ratios of IMT and MET yielded a significant correlation at 15 min postinjection, while at 60 min postinjection no correlation was found (Fig. 2). This indicates a similarity in the initial transport process of both tracers, while at 60 min postinjection the variable washout IMT especially in gliomas produces considerable differences in the tumor to brain ratios of IMT and MET. The similarity in the initial transport process of the tracers also is confirmed by the significant correlation of the K_1 values for IMT and the K_1 values of MET. Since IMT uptake can only be explained by a transport process, this result gives additional support to the hypothesis that transport phenomena play an important role for the increased accumulation of large neutral amino acids in gliomas (8,9,27). A PET study with L-[^{18}F]fluoro-tyrosine, an amino acid analog that is incorporated into protein (28), showed that the difference of uptake between gliomas and normal brain was due to an increase of K_1 , while the rate constant k_3 describing binding to the metabolic compartment was not altered or even decreased in gliomas (11).

The visual comparison of the IMT SPECT and MET PET scans showed no obvious discrepancies in spread and shape of the tracer-accumulating tumor area. Therefore, IMT SPECT appears to have similar diagnostic potentials as MET PET for the delineation of intracerebral gliomas. For MET, many studies have shown larger tumor sizes than CT or MRI and that amino acid PET is better suited to define tumor tissue (1–4,6).

It, however, has to be kept in mind that results concerning tumor to brain ratios from static IMT SPECT scans (15–60 min postinjection) may be different from the results obtained by MET PET due to variable washout of IMT.

A frequently asked question is whether the increased tracer accumulation of IMT and MET in brain tumors is due to a disruption of the blood-brain barrier. Since large neutral amino acids also enter normal brain tissue, a disruption of blood-brain barrier, in other words, contrast enhancement in CT scans, is not a prerequisite for intratumoral amino acid accumulation. This has been shown for MET (1,2,9,10,26) and also for IMT (15,17). Also in this study there are two patients with astrocy-

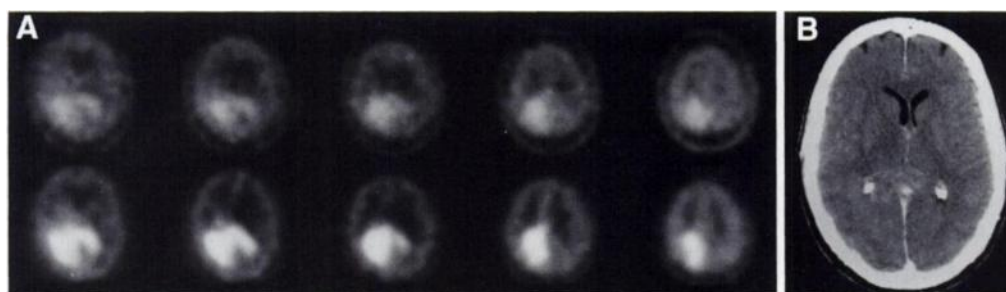


FIGURE 4. (A) Comparison of IMT-SPECT scans (upper row) and MET-PET scans (lower row) (15–60 min postinjection) in a Grade II astrocytoma (Patient 10). Tumor-to-cortex ratio is higher for MET than for IMT, but the extent of the tumor area with increased tracer uptake appears to be similar for IMT and MET. (B) The contrast-enhanced CT scan of the same patient shows no contrast enhancement in the tumor area indicating that there is no blood-brain-barrier disruption.

TABLE 3
Kinetic Rate Constants of IMT and MET

Patient no.	K_1 -IMT tumor	K_1 -IMT brain	Vd-IMT tumor	Vd-IMT brain	K_1 -MET tumor	K_1 -MET brain	Vd-MET tumor	Vd-MET brain
1	0.026 ± 0.001	0.019 ± 0.000	0.84	0.60	0.029	0.016	0.57	0.26
2	0.038 ± 0.005	0.015 ± 0.000	0.59	0.44	0.043	0.024	0.55	0.27
3	0.035 ± 0.001	0.014 ± 0.000	0.71	0.45	0.033	0.012	1.33	0.45
4	0.021 ± 0.001	0.016 ± 0.000	0.81	0.54	0.027	0.015	0.52	0.25
5	0.053 ± 0.001	0.017 ± 0.001	1.14	0.47	0.027	0.015	1.55	0.47
6	0.046 ± 0.002	0.019 ± 0.002	0.94	0.82	0.043	0.020	1.11	0.50
7	0.035 ± 0.002	0.015 ± 0.001	0.75	0.48	0.049	0.05	0.81	0.38
8	0.034 ± 0.001	0.020 ± 0.001	1.15	0.63	0.036	0.020	1.04	0.50
9	0.094 ± 0.006	0.043 ± 0.005	0.99	0.62	0.077	0.033	2.58	1.22
10	0.064 ± 0.002	0.021 ± 0.001	1.52	0.75	0.074	0.023	0.66	0.25
mean	0.044	0.020	0.94	0.58	0.044	0.019	1.07	0.45
s.d.	0.021	0.008	0.27	0.13	0.018	0.006	0.64	0.29

$p < 0.01$ $p < 0.01$ $p < 0.01$ $p < 0.01$

toma Grade II (Patient 5 in Fig. 3, Patient 10 in Fig. 4) exhibiting no contrast enhancement in the CT scan, which showed increased uptake for MET as well as for IMT.

Study Limitations

A number of methodological problems have to be mentioned concerning the absolute values of the rate constants given in this study. Due to the lack of scatter correction and inaccurate attenuation correction inherent with the SPECT method, the absolute K_1 values for IMT must be considered with caution. Furthermore, the plasma input functions for the dynamic SPECT and PET studies were corrected for the non-IMT and non-MET radioactivity using standard values taken from the literature. This ignores the interindividual variability in the metabolism of MET (29) and presumably of IMT. Also, it has to be considered that, in principle, K_1 and K_i are different measures. K_1 describes tracer transport from plasma to tissue, while K_i gives the net tracer influx, which includes plasma to tissue transport, protein synthesis and other intracellular binding. A close coupling of MET transport and intracellular binding, however, has been reported (26), so that the measured K_i value of MET appears to be at least representative for MET transport.

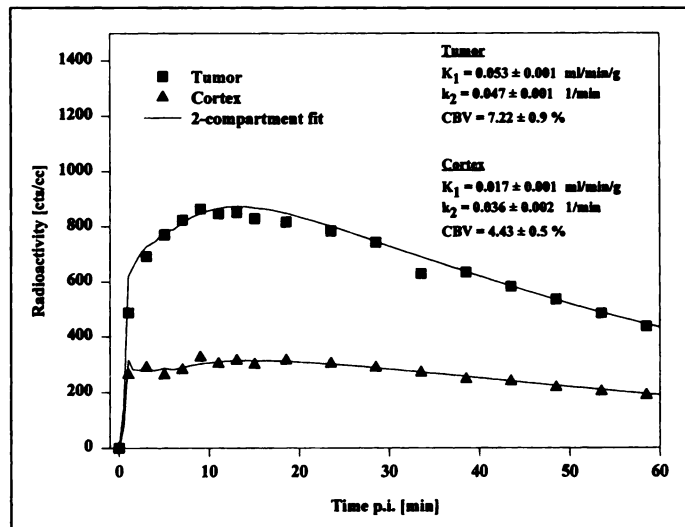


FIGURE 5. Time-activity curves of IMT radioactivity in the tumor and brain of Patient 5. Nonlinear least-square fits to the IMT data using K_1 , k_2 and CBV as fit parameters show satisfactory fits to the data. Addition of k_3 to the fit procedure yielded small values for k_3 without a remarkable improvement of the fit.

CONCLUSION

IMT and MET uptake in gliomas appears to be similar in the early, transport dominated phase. Differences in tumor to brain ratios for both tracers within the first hour postinjection are mainly caused by the variable washout of IMT and to a lesser extent by differences in the initial transport process. Tumor imaging and the delineation of gliomas by IMT SPECT are similar to that of MET PET. Thus, IMT SPECT is a promising method for the evaluation of tumor infiltration and biologic activity of gliomas.

ACKNOWLEDGMENTS

We thank B. Hamacher for assistance in patient studies and data analysis, W. Roden and H. Apelt for technical assistance in the radiosynthesis of L-3-[¹²³I]Iodo- α -methyltyrosine and [methyl-¹¹C]-L-methionine, M. Grosse-Ruyken, L. Leiberts, R. Dahlhoff and M. Griebmeier for assistance with the dynamic SPECT acquisitions, T. Ganslandt for software development for PET data transfer, L. Theelen for PET acquisitions, K. Altman for kindly

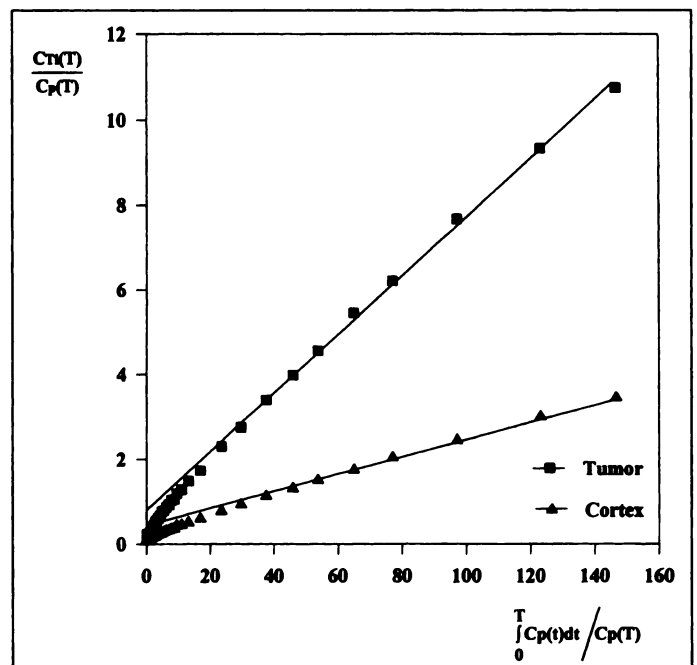


FIGURE 6. Patlak plot to the MET data of the tumor and brain of Patient 10. $C_{T_i}(T)$ is the total amount of radioactivity in the tissue at time T and $C_p(T)$ is the tracer concentration in the plasma at time T.

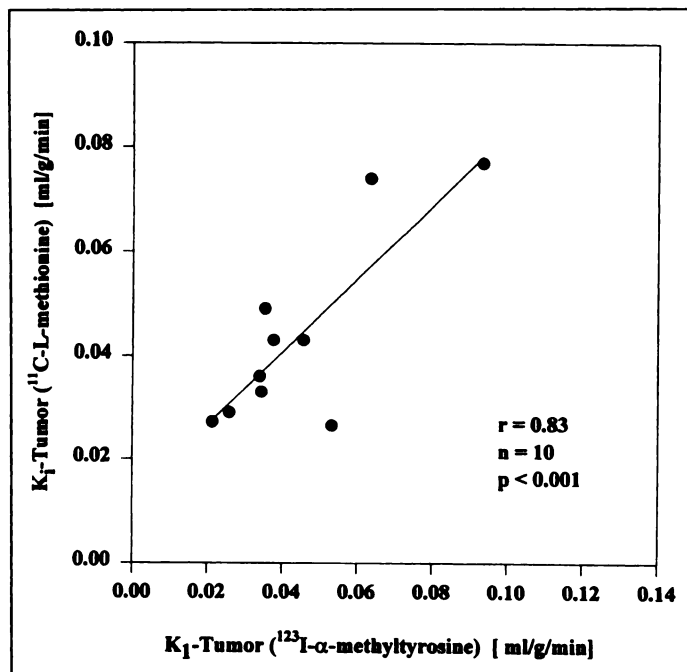


FIGURE 7. Comparison of K_1 values of ^{123}I - α -methyltyrosine and K_1 values of ^{11}C -L-methionine in cerebral gliomas ($n = 10$). There is a significant correlation of both parameters indicating that tracer transport of IMT and MET is similar.

reviewing the manuscript and D. Beaujean for administrative assistance.

REFERENCES

- Bergström M, Collins VP, Ehrin E, et al. Discrepancies in brain tumor extent as shown by computed tomography and positron tomography using ^{68}Ga -EDTA, ^{11}C -glucose and ^{11}C -methionine. *J Comput Assist Tomogr* 1983;7:1062-1066.
- Ericson K, Lilja A, Bergström M, et al. Positron emission tomography with (^{11}C)Methyl-L-methionine, (^{11}C)D-glucose and [^{68}Ga]EDTA in supratentorial tumors. *J Comput Assist Tomogr* 1985;9:683-689.
- Moskin M, von Holst H, Bergström M, et al. Positron emission tomography with ^{11}C -L-methionine and X-ray computed tomography of intracranial tumors compared with histopathologic examination of multiple biopsies. *Acta Radiologica* 1987;28:673-681.
- Moskin M, Ericson K, Hindmarsh T, et al. Positron emission tomography compared with MRI and CT in supratentorial gliomas using multiple stereotactic biopsies as reference. *Acta Radiologica* 1989;30:225-323.
- Derlon JM, Boudet C, Bustany P, et al. [^{11}C]L-methionine uptake in gliomas. *Neurosurgery* 1989;25:720-728.
- Ogawa T, Shishido F, Kanno I, et al. Cerebral glioma: evaluation with methionine PET. *Radiology* 1993;186:45-53.
- Coleman RE, Hoffmann JM, Hanson MW, Sostman HD, Schold SC. Clinical application of PET for the evaluation of brain tumors. *J Nucl Med* 1991;32:616-622.

- Schober O, Meyer G-J, Stolke D, Hundeshagen H. Brain tumor imaging using C-11-labeled L-methionine and D-methionine. *J Nucl Med* 1985;26:98-99.
- Bergström M, Lundquist H, Ericson K, et al. Comparison of the accumulation kinetics of L-(methyl- ^{11}C)-methionine and D-(methyl- ^{11}C)-methionine in brain tumors studied with positron emission tomography. *Acta Radiol* 1987;28:225-229.
- Bergström M, Ericson K, Hagenfeldt L, et al. PET study of methionine accumulation in glioma and normal brain tissue: competition with branched chain amino acids. *J Comput Assist Tomogr* 1987;11:208-213.
- Wienhard K, Herholz K, Coenen HH, et al. Increased amino acid transport into brain tumors measured by PET of L-[2- ^{18}F]fluoro-tyrosine. *J Nucl Med* 1991;32:1338-1346.
- Tisljar U, Kloster G, Ritzl F, Stöcklin G. Accumulation of radioiodinated L- α -methyltyrosine in pancreas of mice: concise communication. *J Nucl Med* 1979;20:973-976.
- Kloster G, Bockslaff H. L-3- ^{123}I - α -methyltyrosine for melanoma detection: a comparative evaluation. *Int J Nucl Med Biol* 1982;9:259-269.
- Biersack HJ, Coenen HH, Stöcklin G, et al. Imaging of brain tumors with L-3-[^{123}I]iodo- α -methyltyrosine and SPECT. *J Nucl Med* 1989;30:110-112.
- Langen K-J, Coenen HH, Roosen N, et al. SPECT studies of brain tumors with L-3-[^{123}I]iodo- α -methyltyrosine: comparison with PET, ^{124}IMT and first clinical results. *J Nucl Med* 1990;31:281-286.
- Kawai K, Fujibayashi Y, Saji H, et al. A strategy for the study of cerebral amino acid transport using I-123-labeled amino acid radiopharmaceutical: 3-iodo- α -methyl-L-tyrosine. *J Nucl Med* 1991;32:819-824.
- Langen K-J, Roosen N, Coenen HH, et al. Brain and brain tumor uptake of L-3-[^{123}I]iodo- α -methyl tyrosine: competition with natural L-amino acids. *J Nucl Med* 1991;32:1225-1228.
- Oldendorf WH. Saturation of amino acid uptake by human brain tumor demonstrated by SPECT [Editorial]. *J Nucl Med* 1991;32:1229-1230.
- Krummeich C, Holschbach M, Stöcklin G. Direct electrophilic radioiodination of tyrosine analogs: their in vivo stability and brain uptake in mice. *Appl Rad Isot* 1994;42:929-935.
- Chang LT. A method for attenuation correction in radionuclide computed tomography. *IEEE Trans Nucl Sci* 1978;25:638-643.
- Rota Kops E, Herzog H, Schmidt A, et al. Performance characteristic of an eight-ring whole-body PET scanner. *J Comput Assist Tomogr* 1990;14:437-445.
- Lundquist H, Stålnacke CG, Långström B, Jones B. Labeled metabolites in plasma after intravenous administration of ^{11}C -[^3H]methionine. In: Greitz T, Ingvar DH, Widén L, eds. *The metabolism of the human brain studied with positron emission tomography*. New York: Raven Press; 1985:233-240.
- Koeppel RA, Mangner T, Betz AL, et al. Use of [^{11}C]aminocyclohexanecarboxylate for the measurement of amino acid uptake and distribution volume in human brain. *J Cereb Blood Flow Metab* 1990;10:727-739.
- Meyer GJ, van den Hoff J, Burchert W, Hundeshagen H. Approaches to quantitative analysis of amino acid transport and metabolism. In: Mazoyer BM, Heiss WD, Comar D, eds. *PET studies on amino acid metabolism and protein synthesis*. Boston, MA: Kluwer Academic Publishers; 1993:183-196.
- Patlak CS, Blasberg RG, Fenstermacher JD. Graphical evaluation of blood to brain transfer constants from multiple time uptake data. *J Cereb Blood Flow Metab* 1983;3:1-7.
- Ericson K, Blomqvist G, Bergström M, Eriksson L, Stone-Elander S. Application of a kinetic model on the methionine accumulation in intracranial tumors studied with positron emission tomography. *Acta Radiol* 1987;28:505-509.
- Ishiwata K, Kubota K, Murakami M, et al. Re-evaluation of amino acid PET studies: can the protein synthesis rates in brain and tumor tissues be measured in vivo? *J Nucl Med* 1993;34:1936-1943.
- Coenen HH, Kling P, Stöcklin G. Cerebral metabolism of L-[2- ^{18}F]fluoro-tyrosine, a new PET tracer of protein synthesis. *J Nucl Med* 1989;30:1367-1372.
- Hatazawa J, Ishiwata K, Itoh M, et al. Quantitative evaluation of L-[methyl- ^{11}C]methionine uptake in tumor using positron emission tomography. *J Nucl Med* 1989;30:1809-1813.

Bilateral Axillary Lymph Node Uptake of Radiotracer During Lower Extremity Lymphoscintigraphy

Douglas M. Howarth and Douglas A. Collins
Department of Nuclear Medicine, Mayo Clinic, Rochester, Minnesota

Lymphoscintigraphy is a useful technique for the evaluation of lymphatic function in the presence of limb swelling. The authors report a case where proximal lower limb and genital swelling in a 23-yr-old man was investigated by lymphoscintigraphy. The patient

had a history of previous surgery and subsequent infection in the affected groin. Lower limb lymphoscintigraphy showed features of an unusual lymphatic drainage pattern that most likely represented adaptation to chronic lymphatic insufficiency. The drainage pattern was characterized by marked dermal backflow pattern, aberrant lymph node uptake in the abdomen and chest and unexpected avid radiotracer uptake in the axillae bilaterally.

Received May 2, 1996; revision accepted Aug. 1, 1996.
For correspondence or reprints contact: Douglas M. Howarth, MD, Dept. of Nuclear Medicine, John Hunter Hospital, Locked Bag No. 1, Hunter Regional Mail Centre, Newcastle NSW 2310, Australia.

J Nucl Med 1997; 38:522-525